Breast Cancer Res Treat (2016) 160:51–59
DOI 10.1007/s10549-016-3972-z

CLINICAL TRIAL

ANG1005 for breast cancer brain metastases: correlation between ^{18}F-FLT–PET after first cycle and MRI in response assessment

C. C. O'Sullivan[1,2] · M. Lindenberg[1] · C. Bryla[1] · N. Patronas[1] · C. J. Peer[1] · L. Amiri-Kordestani[1] · N. Davarpanah[1] · E. M. Gonzalez[1] · M. Burotto[1,3] · P. Choyke[1] · S. M. Steinberg[1] · D. J. Liewehr[1] · W. D. Figg[1] · T. Fojo[1,4] · S. Balasubramaniam[1] · S. E. Bates[1,4]

Received: 20 June 2016 / Accepted: 2 September 2016 / Published online: 12 September 2016

Abstract

Purpose Improved therapies and imaging modalities are needed for the treatment of breast cancer brain metastases (BCBM). ANG1005 is a drug conjugate consisting of paclitaxel covalently linked to Angiopep-2, designed to cross the blood–brain barrier. We conducted a biomarker substudy to evaluate ^{18}F-FLT–PET for response assessment.

Methods Ten patients with measurable BCBM received ANG1005 at a dose of 550 mg/m^2 IV every 21 days. Before and after cycle 1, patients underwent PET imaging with ^{18}F-FLT, a thymidine analog, retention of which reflects cellular proliferation, for comparison with gadolinium-contrast magnetic resonance imaging (Gd-MRI) in brain metastases detection and response assessment. A 20 % change in uptake after one cycle of ANG1005 was deemed significant.

Results Thirty-two target and twenty non-target metastatic brain lesions were analyzed. The median tumor reduction by MRI after cycle 1 was −17.5 % ($n = 10$ patients, lower, upper quartiles: −25.5, −4.8 %) in target lesion size compared with baseline. Fifteen of twenty-nine target lesions (52 %) and 12/20 nontarget lesions (60 %) showed a ≥20 % decrease post-therapy in FLT–PET SUV change (odds ratio 0.71, 95 % CI: 0.19, 2.61). The median percentage change in SUV_{max} was −20.9 % ($n = 29$ lesions; lower, upper quartiles: −42.4, 2.0 %), and the median percentage change in SUV_{80} was also −20.9 % ($n = 29$; lower, upper quartiles: −49.0, 0.0 %). Two patients had

✉ C. C. O'Sullivan
osullivan.ciara@mayo.edu

M. Lindenberg
maria.lindenberg@nih.gov

C. Bryla
christine.bryla@nih.gov

N. Patronas
npatronas@cc.nih.gov

C. J. Peer
cody.peer@nih.gov

L. Amiri-Kordestani
laleh.amirikordestani@fda.hhs.gov

N. Davarpanah
nicole.davarpanah@nih.gov

E. M. Gonzalez
edith.gonzalez@fda.hhs.edu

M. Burotto
mburotto@alemana.cl

P. Choyke
pchoyke@mail.nih.gov

S. M. Steinberg
steinbes@mail.nih.gov

D. J. Liewehr
liewehrd@mail.nih.gov

W. D. Figg
wf13e@nih.gov

T. Fojo
atf2116@cumc.columbia.edu

S. Balasubramaniam
sanjeeve.balasubramaniam@fda.hhs.gov

S. E. Bates
seb2227@cumc.columbia.edu

[1] National Cancer Institute, Bethesda, MD, USA

[2] Department of Medical Oncology, Mayo Clinic, 200 1st Street SW, Rochester, MN 55905, USA

[3] Pontificia Universidad Católica de Chile, Santiago, Chile

[4] Columbia University, New York, NY, USA

confirmed partial responses by PET and MRI lasting 6 and 18 cycles, respectively. Seven patients had stable disease, receiving a median of six cycles.
Conclusions ANG1005 warrants further study in BCBM. Results demonstrated a moderately strong association between MRI and ^{18}F-FLT–PET imaging.

Keywords Breast cancer brain metastases · ANG1005 · ^{18}F-FLT–PET · MRI brain

Introduction

Approximately 10–30 % of patients with breast cancer develop brain metastases, which are associated with the shortest median survival compared to other sites of metastatic spread [1]. Management of these patients is challenging; the main issues are selective permeability of chemotherapy and targeted therapies across the blood–brain barrier (BBB) and resistance to standard treatments. Additionally, as traditional imaging modalities have limitations in assessing response to treatment [2], both novel treatments and imaging techniques are urgently needed.

ANG1005 (GRN1005) is a Cremophor-free peptide–drug conjugate consisting of three molecules of paclitaxel, covalently linked to a peptide vector, Angiopep-2 [3, 4], which was designed to cross the BBB and enter tumor cells via low-density lipoprotein receptor-related protein-1 (LRP-1)-mediated transcytosis [5–7]. ANG1005 is activated in tumor cells following cleavage by intracellular esterases, releasing conjugated paclitaxel from the Angiopep-2 peptide backbone. Paclitaxel can then bind tubulin and function to stabilize microtubules [3]. The activity of ANG1005 on brain tumors was evaluated using intracerebral human tumor models in nude mice; preclinical studies showed that the brain's uptake of ANG1005 was approximately 86-fold greater than paclitaxel [3, 8]. Regina et al. demonstrated antineoplastic potency for ANG1005 similar to that of paclitaxel against human cancer cell lines, and a more potent inhibition of intracerebral human tumor xenografts in murine models than paclitaxel [3]. Further, data from multi-center phase I trials showed ANG1005 was associated with manageable toxicity and activity in patients with brain metastases from advanced solid tumors and recurrent malignant gliomas [4, 9], leading the way for phase II studies in patients with breast cancer brain metastases (BCBM).

Magnetic resonance imaging (MRI) is the gold standard in the assessment and monitoring of patients with brain metastases [10]. While gadolinium (Gd)-enhanced MRI scans demarcate individual tumors and their surrounding anatomy, these studies are limited in that gadolinium enhancement of brain tumors mainly reflects impairment, or leakiness, of the BBB, and interventions that affect BBB permeability alter gadolinium enhancement [11]. Positron emission tomography (PET) is a functional imaging modality that uses radioactive tracers to provide information relevant to different cellular and molecular events [12]. 3′-deoxy-3′-18F fluorothymidine (^{18}F-FLT) is a thymidine analog that acts as a chain terminator in the synthesis of DNA; its retention reflects DNA synthesis [13]. It has been studied as a radiolabeled imaging probe for the assessment of cellular proliferation in malignant tumors [12]. In general, ^{18}F-FLT appears to offer little benefit over standard ^{18}F-FDG for diagnosis and staging of different cancers [14–21], but appears to be more sensitive than ^{18}F-FDG in detecting central nervous system (CNS) tumors [22, 23]. A study in 25 patients with newly diagnosed or recurrent gliomas showed that ^{18}F-FLT was more sensitive than ^{18}F-FDG for detection of high-grade tumors, and this finding was associated with a higher correlation between tumor uptake and Ki-67 index for ^{18}F-FLT than for ^{18}F–FDG [24].

The National Cancer Institute (NCI) participated in a phase II multi-center trial to assess the efficacy of ANG1005 in the treatment of BCBM. As ^{18}F-FLT–PET has shown utility in assessing treatment response in breast cancer patients [25, 26], we conducted an imaging substudy alongside the ongoing multiple-cycle efficacy phase II study.

Methods

Patients

Eligible patients had to have histologically or cytologically confirmed breast cancer with known hormone receptor (HR) and HER2 status (HER2-positive tumors were defined as having an immunohistochemistry score of 3+ or evidence of gene amplification according to FISH). Patients had to have *at least one* radiologically confirmed and metastatic brain lesion ($\geq$1.0 cm in longest diameter by Gd-MRI of brain) that had not undergone radiosurgery. Prior whole-brain radiotherapy (WBRT) was allowed, if >28 days prior to study enrollment. Corticosteroids and anticonvulsants (not enzyme-inducing antiepileptic drugs), if required, had to be at stable doses for >5 days before baseline Gd-MRI brain and $\geq$5 days prior to the first dose of ANG1005. Patients with HER2-positive disease already on trastuzumab were recommended to continue the same, provided standard of care criteria were met regarding adequate left ventricular ejection fraction (LVEF) [27]. Exclusion criteria included grade $\geq$2 neuropathy, CNS disease requiring immediate neurosurgical intervention, and known leptomeningeal disease. The NCI Clinical

Cancer Research Institutional Review Board approved the study protocol.

Study design

This was a single institution first-cycle imaging substudy conducted as part of a phase II, multi-center, open-label trial of ANG1005 alone or in combination with trastuzumab in patients with BCBM (NCT01480583). Our primary objective was to determine whether one cycle of ANG1005 therapy is associated with a significant change in ^{18}FLT–PET uptake. Secondary objectives included determining whether percentage change in ^{18}FLT–PET/CT uptake after 1 cycle of ANG1005 is correlated with intracranial tumor response on MRI.

Administration of study treatment

Patients received ANG1005 therapy at a dose of 550 mg/m^2 IV every 21 days until intracranial disease progression or unacceptable toxicity. Premedication was not required. Six mg of Neulasta subcutaneously was administered 24 h after each infusion of ANG1005 to all the patients. Adverse events were recorded every 3 weeks and graded according to the NCI Common Toxicity Criteria for Adverse Events (CTCAE), version 4.0.

Efficacy assessments

Patients had to have measurable disease present at baseline, have received at least one cycle of therapy, and have had their disease re-evaluated before they could be considered evaluable for response. This was determined using Response Evaluation Criteria in Solid Tumors (RECIST) v1.1 for peripheral disease [28], and intracranial disease was assessed using modified RECIST criteria (CNS RECIST v1.1) [28]. MRI images were centrally reviewed and lesions measured by a neuroradiologist (coauthor NP). Patients underwent ^{18}F-FLT PET/CT imaging before and after the first cycle of therapy of ANG1005. Dynamic 3D PET emission brain imaging was performed over 30 min, and then a static whole-body PET scan at 1 h post-injection was conducted. With regards to the ^{18}F-FLT PET/CT scan, volumes of interest were drawn in target brain metastases. The maximum pixel value was taken as the maximum standard uptake value, or SUV_{max}, and the tumor-to-normal (T:N) ratio was calculated. The SUV_{80} was also determined, the 80 % threshold reflecting the average value of the maximum 20 % pixels. The percentage change before and after cycle 1 was calculated, with a 20 % change considered to be significant. As the historical intracranial overall response rate (ORR) in the target population was assumed to be <10 %, a response rate of ≥20 % would indicate that GRN1005 has clinically meaningful activity in this patient population. Changes in FLT–PET were assessed after the first cycle of therapy. Patients underwent MRI brain scans after every two cycles of therapy until disease progression or withdrawal from study. Results from the Phase II study, which enrolled 61 patients, will be reported elsewhere.

Statistical analysis

The primary endpoint on which the sample size for this portion of the study was based on was to determine if there was a change in the FLT–PET uptake as measured by SUV after ANG1005 treatment compared to baseline. We planned to enroll ten patients at our site in order to have 80 % power to detect a one standard deviation change in the level of SUV after treatment compared to before treatment using a 0.05 alpha level two-tailed paired t test. To estimate the degree of correlation between the four FLT–PET variables with the three MRI variables, we performed a Spearman rank correlation analysis on the data; prior to analysis, the median value of each PLT-PET variable was calculated for each of the ten patients (the sample size was 9 or 10 for each estimated correlation coefficient). Strong associations were as follows: $|r| > 0.7$, moderate association: $0.5 < |r| < 0.7$, moderate to weak association: $0.3 < |r| < 0.5$, and weak association: $|r| < 0.3$. Confidence limits (95 %) for the correlation coefficients are reported with each Spearman correlation coefficient (r). Correlation analyses were limited to individual patient medians, not lesions, as lesions from the same individual could not be considered independent of one another. However, plots of individual target lesions were made for presentation purposes. All statistical analyses were performed using SAS (R) version 9.3. All other evaluations were performed with exploratory intent and reported as being hypothetical generating in view of the pilot nature of the study.

Results

Patient characteristics

Patient characteristics and details of prior treatment are listed in Table 1. Median age for all ten patients was 52.5 years. The median duration since the original diagnosis of brain metastases was 12.5 months (minimum, maximum 0.5–25 months). Patients received a median of 3 prior systemic treatments in the metastatic setting prior to study enrollment (minimum, maximum 1–11). All ten patients (100 %) had prior taxane-based treatment.

Two of the ten patients previously had a craniotomy before enrolling in study (2/10; 20 %), and nine of the ten patients had received either whole-brain radiotherapy (WBRT) or stereotactic radiotherapy (SRS) (9/10; 90 %). Five of the ten patients (50 %) had HER2-positive disease.

Toxicity and dose intensity

ANG1005 ± trastuzumab was generally well tolerated. All ten patients (100 %) had hematological toxicity. Six of these patients had grade ≥3 neutropenia. Four patients (40 %) had grade ≥3 lymphopenia, and two patients (20 %) had grade ≥3 thrombocytopenia. Regarding non-hematologic adverse events, the most common grade 1 and 2 adverse events were fatigue (40 %), alopecia (30 %), vomiting (20 %), rash (20 %), and nausea (20 %). Grade ≥3 adverse events included vomiting (20 %), febrile neutropenia (20 %), nausea (10 %), diarrhea (10 %), and fatigue (10 %).

Results by MRI

Tumor reductions as defined by MRI using the modified response evaluation criteria in solid tumors (RECIST) for the central nervous system (CNS) had a median decrease of 17.5 % ($n = 10$ patients; lower, upper quartiles: −25, −4.8 %) in lesion size compared to baseline (Table 2). Two patients had confirmed partial responses (PR) lasting 6 and 18 cycles, respectively. Seven patients had stable disease (SD), receiving a median of six cycles. One patient had progressive disease (PD) after receiving three cycles.

Analysis of intracranial response by FLT–PET

Target lesions chosen by MRI evaluation were then reviewed for FLT–PET quantitation; additional clearly visible lesions were considered nontarget lesions, and SUV for those lesions were interpreted separately. Of the 32 target (T) and 20 nontarget (NT) metastatic brain lesions measured by MRI, 29 T and 20 NT were measured by FLT–PET. At 30 min, the SUV_{MAX} ranged from 0.8 to 6.3

Table 1 Demographics and prior therapy use

	Total ($N = 10$)
Age, median years (minimum, maximum)	52.5 (30–63)
Duration since initial diagnosis of breast cancer, median years (minimum, maximum)	5.5 (1.3–16.5)
Duration since initial diagnosis of brain metastases, median months (minimum, maximum)	12.5 (0.5–25)
HER2 status *n* (%)	
HER2−	5 (50 %)
HER2+	5 (50 %)
ER and PR status *n* (%)	
ER+, PR+	3 (30 %)
ER+, PR−	0 (0 %)
ER−, PR+	2 (20 %)
ER−, PR−	5 (50 %)
Prior intracranial radiotherapy *n* (%)	
WBRT+, SRS+	2 (25 %)
WBRT+, SRS−	3 (38 %)
WBRT−, SRS+	0 (%)
WBRT−, SRS−	3 (38 %)
External radiation	1 (13 %)
Prior surgery *n* (%)	
Craniotomy	2 (20 %)
Prior systemic therapies in metastatic setting, median (minimum, maximum)	3 (1–11)
Prior taxane therapy *n* (%)	10 (100 %)
Taxane given in adjuvant setting only	4 (40 %)
Taxane given in metastatic setting only	3 (20 %)
Taxane given in both the adjuvant and metastatic setting	3 (30 %)

HER2 human epidermal growth factor receptor 2, *ER* estrogen receptor, *PR* progesterone receptor, *WBRT* whole-brain radiotherapy, *SRS* stereotactic radiosurgery

Table 2 Individual patients' response to treatment

Patient #	Hormone receptor status	# Cycles received	Response	Best MRI response target only (%)	% Change FLT–PET (SUVmax) *T* + *NT*	% Change FLT–PET (SUVmax) target only	% Change FLT–PET (SUV_{80}) *T* + *NT* (%)	% Change FLT–PET (SUV_{80}) target only (%)
1	ER−/PR−/HER2−	2	SD	−4.8	5.1 % (3)	30 % (2)	29	37
2	ER−/PR−/HER2+	6	SD	−20	−11 % (3)	NA (–)	−14	NA
3	ER−/PR−/HER2+	8	SD	−2.7	−5.9 % (4)	0.5 % (3)	−6.7	−1.2
4	ER+/PR+/HER2−	6	SD	−25	−33 % (5)	−33 % (3)	−44	−44
5	ER−/PR−/HER2−	6	PR	−62	−68 % (1)	−68 % (1)	−67	−67
6	ER−/PR−/HER2−	3	PD	−15	28 % (9)	34 % (4)	21	32
7	ER+/PR+/HER2+	18	PR	−57	−51 % (7)	−56 % (5)	−51	−58
8	ER+/PR+/HER2+	7	SD	−22	−38 % (7)	−35 % (4)	−42	−37
9	ER−/PR+/HER2+	4	SD	4.8	−7.0 % (7)	−6.0 % (4)	−7.0	−6.7
10	ER−/PR−/HER2−	3	SD	−10	−18 % (3)	−18 % (3)	−21	−21

Pt patient, *#* number, *ER* estrogen receptor, *PR* progesterone receptor, *HER2* human epidermal growth factor receptor 2, *SUV* standard uptake volume, *SD* stable disease, *PR* partial response, *PD* progressive disease, *T* target, *NT* nontarget, *NA* unable to assess, number of lesions (*n*)

at baseline, mean 3.0. In total, 15/29 target lesions and 12/20 nontarget lesions showed a $\geq$20 % decrease post-therapy (odds ratio 0.71; 95 % CI 0.19, 2.61). Figure 1 depicts a waterfall plot for the best response for each patient and for percent reduction of the individual target ($n = 29$) lesions. The median percentage change in SUV_{max} was −20.9 % ($n = 29$ lesions; lower, upper quartiles: −42.4 , 2.0 %), and for SUV_{80} was also −20.9 % ($n = 29$; lower, upper quartiles: −49.0, 0.0 %). The tumor-to-normal (*T:N*) ratios ranged from 3.3 to 45.1, (mean 15.0) at baseline and after one cycle; the median percent change in *T:N* was −21.3 % ($n = 29$; lower, upper quartiles: −23.8, −9.9 %).

Association between MRI and FLT–PET imaging

There was a moderately strong association (Spearman $r > 0.7$) between MRI and FLT–PET imaging based on percent change in SUV_{MAX} between baseline and post cycle 1 (Table 3). The additional FLT–PET parameters were at least moderately associated with each other, as indicated by the similar Spearman r values ($r = 0.63$ or $r = 0.80$) for each association. Figure 1a depicts the best MRI response versus percentage change in SUV_{MAX} (same data as in Table 3). The percentage change in SUV_{MAX} in measurable individual target lesions appeared to be related to the median of individual lesion maximum response (Fig. 1b); however, a Spearman *r* could not be assigned due to lack of independent samples (29 lesions from 9 patients). The data shown in Fig. 1 **a**–**b** appeared to follow a nonlinear pattern; thus, a locally weighted scatterplot smoothing (LOESS) regression was used to visualize the relationship (Fig. 1c), and a linear regression line is shown for comparison purposes. This pattern may be due to a small sample size, particularly as FLT–PET percent changes approach positive territory. There appears to be a linear pattern where both MRI and FLT–PET measured negative percent changes in tumor uptake (indicating tumor shrinkage from one cycle of ANG1005). Figure 2 depicts baseline MRI scans and ^{18}FLT PET scans pre- and post one cycle of ANG1005 for patients 5–7. Caution should be used when interpreting these results, as sample size is small.

Discussion

This report shows the impact of ANG1005, an agent with activity in BCBM, on the uptake of radiolabeled fluorothymidine. ^{18}F-FLT–PET was performed at baseline and after one cycle of ANG1005, whereas MRI Brain was performed at baseline and after two cycles of ANG1005. Based on the results, ^{18}F-FLT–PET may be a useful tool to predict response in this setting, as it appears to correlate well (Spearman $r > 0.7$) with best MRI response and the median percentage change in FLT–PET by patient. These findings are encouraging, given the lack of effective treatments and accurate imaging modalities for patients with BCBM.

Contrast-enhanced MRI detection of brain metastases represents gadolinium leakage through the BBB, as opposed to actual tumor volume [29, 30]. Pseudoresponse and pseudoprogression are terms describing inaccurate CNS response assessment, and both have been described with conventional MRI imaging. Pseudoresponse is a phenomenon whereby contrast uptake is reduced due to a reduction in vascular permeability, which is seen in patients on steroids or in patients with glioblastoma multiforme (GBM) treated with antiangiogenic agents [31]. On

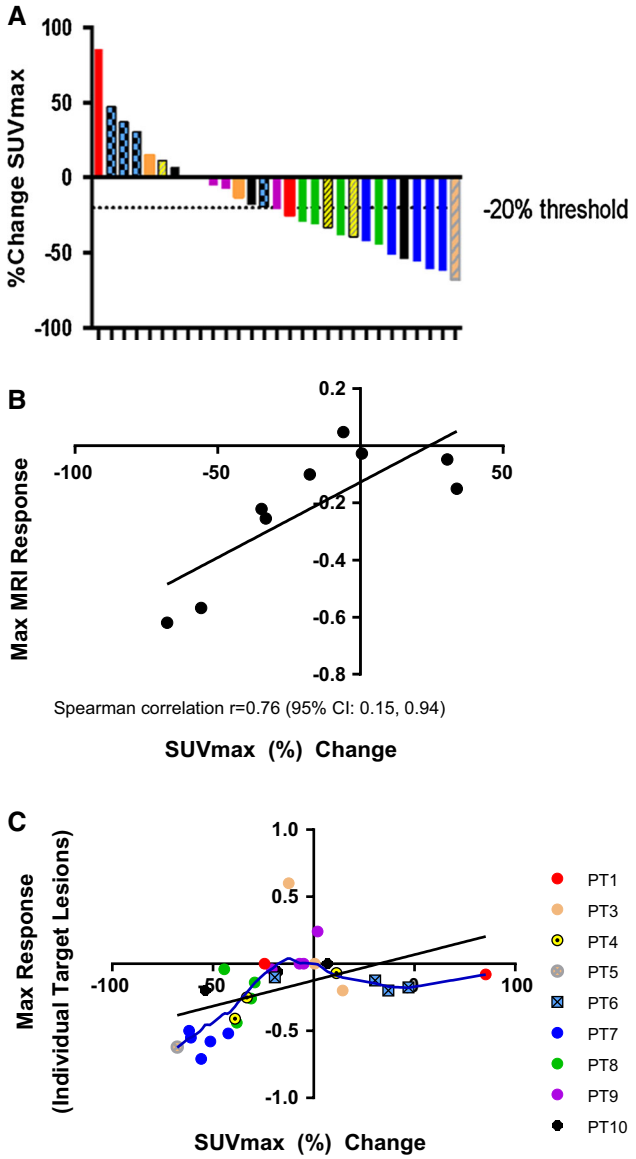

Fig. 1 Comparison of MRI and FLT–PET imaging. **a** Percentage change SUV_{max} versus target lesions only. The 20 % decrease threshold is demarked by a *dashed line*. **b** Median SUV_{MAX} percent change in patients with target lesions ($n = 9$) versus maximum response (same data as in Table 3); in each pane, the *solid black line* is the linear regression fit, with the *dashed lines* representing the 95 % confidence interval. **c** Percentage change median SUV_{MAX} (Target) shown as a waterfall plot (lesions are color-coded by patient to match Fig. 1a). A LOESS (locally weighted scatterplot smoothed) regression (*solid blue line*) was also applied to the data

the other hand, cytotoxic therapy or radiation therapy can cause cell damage and local inflammation, which may increase vascular permeability, resulting in early increases in contrast enhancement, i.e., pseudoprogression [32–34]. Therefore, improved strategies are needed to more accurately determine treatment response in this setting [25].

There is considerable interest for development of ^{18}F-FLT–PET as a cancer imaging biomarker, especially as it is becoming more readily available. Therefore, studies focusing on its mechanism of action and potential clinical applications are important. An advantage of ^{18}F-FLT–PET is that uptake in normal brain parenchyma is low, which allows visualization of brain tumors with high contrast. However, a limitation is that benign lesions disrupting the BBB cannot be distinguished from malignant tumors. Additionally, the extent to which ^{18}F-FLT–PET correlates with proliferative index in different tumor types is variable, as ^{18}F-FLT–PET cannot discriminate between moderately proliferative tumors driven by thymidine salvage from those dependent on de novo thymidine synthesis. However, ^{18}F-FLT–PET accurately quantified the proliferation activity of malignant brain tumors in a study of 25 patients. Research is ongoing; NCT02328300 is assessing ^{18}F-FLT–PET and MRI for the evaluation of pseudoprogression in patients with brain metastases, and NCT01621906 is comparing MRI with ^{18}F-FLT–PET in patients with BCBM receiving whole-brain radiotherapy (WBRT)± the multikinase inhibitor sorafenib. The available evidence suggests that FLT–PET imaging in this setting may

Table 3 Comparisons between MRI versus FLT–PET

MRI variable	FLT–PET variable	*N*	Spearman *r*	95 % CI
Best MRI (*T* only)	SUV_{MAX} %-change	9	0.75	0.13, 0.94
	T_{MAX}:N %-change	9	0.63	−0.09, 0.91
	SUV_{80} %-change	9	0.80	0.24, 0.95
	T_{80}:N %-change	9	0.63	−0.09, 0.91
Best MRI (*T* + *NT*)	SUV_{MAX} %-change	10	0.79	0.29, 0.94
	T_{MAX}:N %-change	10	0.59	−0.10, 0.88
	SUV_{80} %-change	10	0.83	0.38, 0.95
	T_{80}:N %-change	10	0.68	0.06, 0.91
Max response[a]	SUV_{MAX} %-change	9	0.76	0.15, 0.94
	T_{MAX}:N %-change	9	0.66	−0.05, 0.91
	SUV_{80} %-change	9	0.81	0.27, 0.95
	T_{80}:N %-change	9	0.66	−0.05, 0.91

SUV standard uptake volume, *T* target lesion, *NT* nontarget lesion

[a] Based on patient-specific medians of evaluable target lesions (one patient did not have evaluable target lesions)

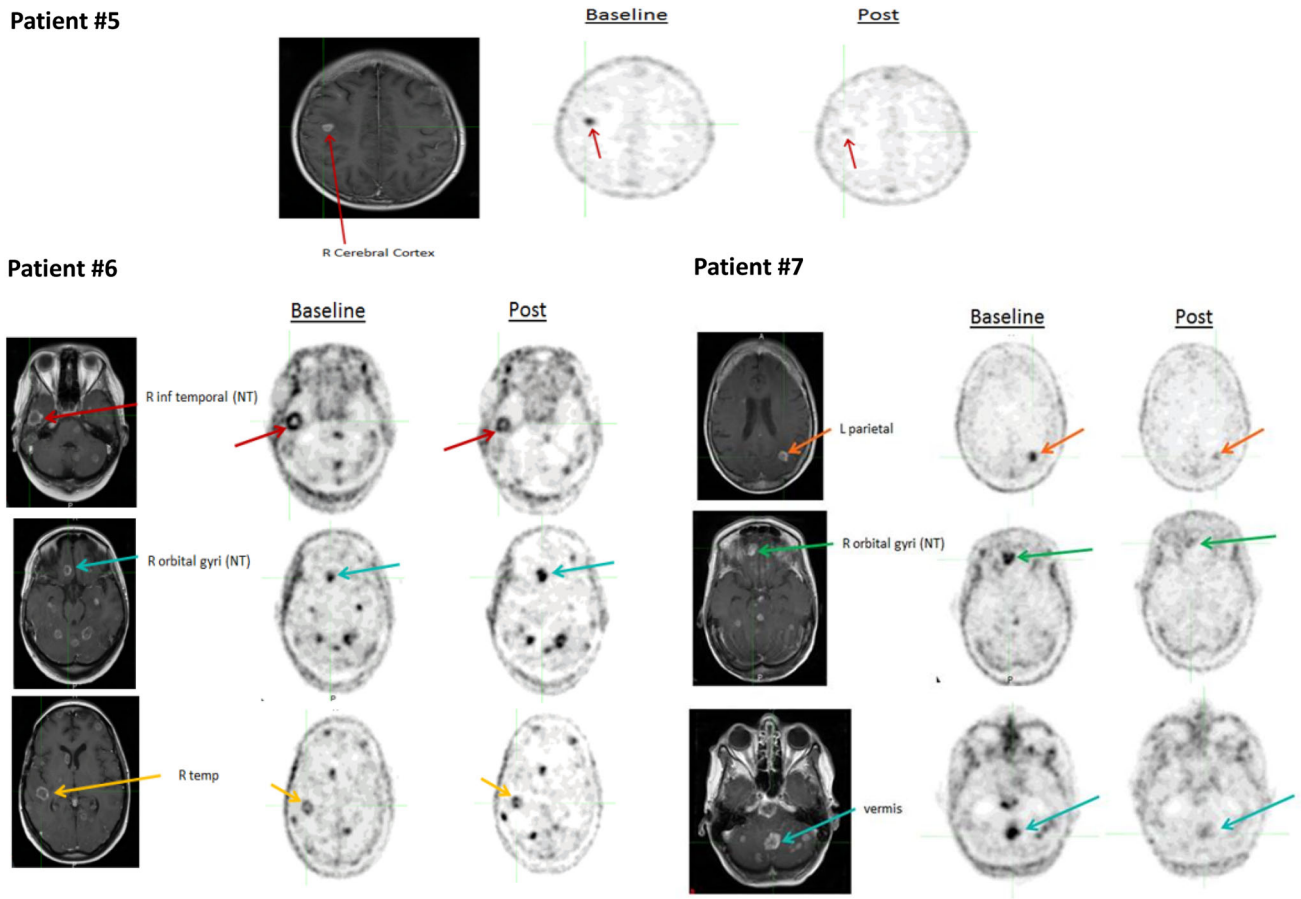

Fig. 2 Responses of individual patients. Baseline MRIs and ^{18}FLT–PET scans pre and post cycle 1 of ANG1005 are presented for each patient. Patients 5 and 7 had a partial response to treatment, and patient 7 remained on study for 18 cycles. Patient 6 had a mixed response, in that some lesions responded (decreased in size by 40–50 %) and some progressed (increased in size by 40–50 %). This illustrates how tumor heterogeneity can impact response assessment and treatment benefit. *R* right, *inf* inferior, *NT* nontarget, *temp* temporal, *L* left

improve response assessment [35, 36]. Our preliminary evaluation of FLT–PET imaging for CNS disease in BCBM suggests that it is a promising tool that could serve as a complementary assessment method, supporting or clarifying MRI findings. We noted a correlation between FLT–PET change after one cycle and ultimate best response ($r = 0.75$) after ANG1005. While these results have to be considered preliminary due to the small size (and the very wide confidence interval), they certainly support an expanded look at the imaging technique. Improving our ability to determine who may be benefiting from therapy is a critical piece in improving the study of new agents in this setting, several of which are in clinical development [37].

Phase I and II clinical studies have demonstrated signs of both CNS and peripheral antitumor activity of ANG1005 in patients with brain metastases from lung and breast cancer [4, 9, 38]. Additionally, ANG1005 received orphan drug designation from the FDA for treatment of GBM in 2014, and for BCBM in March 2015 [39]. In the phase I trial, 5/27 (18.5 %) patients were noted to have a PR, and 11/27 (41 %) had SD at doses $\geq$420 mg/m^2. Our imaging trial was a substudy of a phase II trial conducted by Lin et al., to evaluate the CNS and peripheral antitumor activity of ANG1005 in patients with BCBM [38]. Safety and tolerability of ANG1005 resembled a taxane profile. In the phase II study, 61 patients were treated. For patients who were treated at the 550 mg/m^2 dose, best responses in the CNS were as follows: ten patients had a PR (20 %), 31 patients had SD (61 %), and ten patients had disease progression (20 %). The best observed responses for peripheral disease in this patient group were as follows: one patient had a CR (4 %), seven patients had a PR (25 %), 14 patients had SD (50 %), and six patients had disease progression (21 %). At the 650 mg/m^2 dose, CNS responses were as follows: four patients had a PR (40 %), four patients had SD (40 %), and two patients had PD (20 %). Peripheral response rates for patients treated at this dose were as follows: PR = one patient (25 %), SD = two patients (50 %), and one patient had PD (25 %). Of note, five of the ten patients in our imaging substudy

(50 %) had HER2-positive disease, which may be due to selection bias of patients being enrolled.

ANG1005 is an interesting compound in that it delivers a well-understood and effective anticancer agent both to the CNS and systemically. Paclitaxel also combines well with other anticancer agents, in particular DNA-damaging agents. Studies of ANG1005 in combination with other agents will be an important future direction. Tests have shown that patients do not develop antibodies to ANG1005, even after numerous cycles of treatment in some cases, and patients do not require premedication. Neurocognitive toxicities have not been observed, and systemic toxicities are the well-known effects of paclitaxel [40, 41]. A phase II, open-label, multi-center study of ANG1005 in breast cancer patients with recurrent brain metastases is currently ongoing, but closed to accrual (NCT02048059); the primary outcome measure is intracranial objective response rate (ORR). The trial planned to enroll 56 evaluable patients, and the expected completion date is October 2016. While further studies with ANG1005 should be conducted, the role of Angiopep-2 should also be further explored, as it is possible that conjugation of anticancer agents with this vector could increase their efficacy in the treatment of brain metastases. In summary, therapy for BCBM is an important unmet need, as is assessment of therapeutic outcome. ANG1005 has activity in BCBM, with a manageable toxicity profile. FLT–PET imaging could potentially represent a complementary assessment method, which could improve MRI evaluation of CNS response. Further studies of ANG1005 are warranted, and combination studies should be developed.

Acknowledgments We would like to thank all the patients, their families, the research, and allied health professional staff in the National Cancer Institute for their valuable contributions to this study. ANG1005 was provided by Angiochem, and representatives from the company reviewed the manuscript. None of the authors have a financial relationship with Angiochem or have other relevant conflicts of interest to disclose.

Author contributions Both Susan E. Bates and Antonio T. Fojo had full access to all of the data in the study and took responsibility for the integrity of the data and the accuracy of the data analysis.

Compliance with ethical standards

Conflict of Interest None of the authors have any relevant disclosures.

References

1. Kennecke H, Yerushalmi R, Woods R, Cheang MC, Voduc D, Speers CH et al (2010) Metastatic behavior of breast cancer subtypes. J Clin Oncol 28(20):3271–3277
2. Gempt J, Bette S, Buchmann N, Ryang YM, Forschler A, Pyka T et al (2015) Volumetric analysis of F-18-FET-PET imaging for brain metastases. World Neurosurg 84(6):1790–1797
3. Regina A, Demeule M, Che C, Lavallee I, Poirier J, Gabathuler R et al (2008) Antitumour activity of ANG1005, a conjugate between paclitaxel and the new brain delivery vector Angiopep-2. Br J Pharmacol 155(2):185–197
4. Kurzrock R, Gabrail N, Chandhasin C, Moulder S, Smith C, Brenner A et al (2012) Safety, pharmacokinetics, and activity of GRN1005, a novel conjugate of angiopep-2, a peptide facilitating brain penetration, and paclitaxel, in patients with advanced solid tumors. Mol Cancer Ther 11(2):308–316
5. Demeule M, Currie JC, Bertrand Y, Che C, Nguyen T, Regina A et al (2008) Involvement of the low-density lipoprotein receptor-related protein in the transcytosis of the brain delivery vector angiopep-2. J Neurochem 106(4):1534–1544
6. Demeule M, Regina A, Che C, Poirier J, Nguyen T, Gabathuler R et al (2008) Identification and design of peptides as a new drug delivery system for the brain. J Pharmacol Exp Ther 324(3):1064–1072
7. Bertrand Y, Currie JC, Poirier J, Demeule M, Abulrob A, Fatehi D et al (2011) Influence of glioma tumour microenvironment on the transport of ANG1005 via low-density lipoprotein receptor-related protein 1. Br J Cancer 105(11):1697–1707
8. Thomas FC, Taskar K, Rudraraju V, Goda S, Thorsheim HR, Gaasch JA et al (2009) Uptake of ANG1005, a novel paclitaxel derivative, through the blood-brain barrier into brain and experimental brain metastases of breast cancer. Pharm Res 26(11):2486–2494
9. Drappatz J, Brenner A, Wong ET, Eichler A, Schiff D, Groves MD et al (2013) Phase I study of GRN1005 in recurrent malignant glioma. Clin Cancer Res 19(6):1567–1576
10. Nowosielski M, Radbruch A (2015) The emerging role of advanced neuroimaging techniques for brain metastases. Chin Clin Oncol 4(2):23
11. Ellingson BM, Wen PY, van den Bent MJ, Cloughesy TF (2014) Pros and cons of current brain tumor imaging. Neuro Oncol 16(Suppl 7):vii2–vii11
12. Beadsmoore C, Newman D, MacIver D, Pawaroo D (2015) Positron emission tomography computed tomography: a guide for the general radiologist. Can Assoc Radiol J 66(4):332–347
13. Peck M, Pollack HA, Friesen A, Muzi M, Shoner SC, Shankland EG et al (2015) Applications of PET imaging with the proliferation marker [18F]-FLT. Q J Nucl Med Mol Imaging 59(1):95–104
14. Yamamoto Y, Nishiyama Y, Kimura N, Ishikawa S, Okuda M, Bandoh S et al (2008) Comparison of (18)F-FLT PET and (18)F-FDG PET for preoperative staging in non-small cell lung cancer. Eur J Nucl Med Mol Imaging 35(2):236–245
15. Halter G, Buck AK, Schirrmeister H, Aksoy E, Liewald F, Glatting G et al (2004) Lymph node staging in lung cancer using [18F]FDG-PET. Thorac Cardiovasc Surg 52(2):96–101
16. Cobben DC, Elsinga PH, Hoekstra HJ, Suurmeijer AJ, Vaalburg W, Maas B et al (2004) Is 18F-3′-fluoro-3′-deoxy-L-thymidine useful for the staging and restaging of non-small cell lung cancer? J Nucl Med 45(10):1677–1682
17. Buck AK, Halter G, Schirrmeister H, Kotzerke J, Wurziger I, Glatting G et al (2003) Imaging proliferation in lung tumors with PET: 18F-FLT versus 18F-FDG. J Nucl Med 44(9):1426–1431
18. Francis DL, Visvikis D, Costa DC, Arulampalam TH, Townsend C, Luthra SK et al (2003) Potential impact of [18F]3′-deoxy-3′-fluorothymidine versus [18F]fluoro-2-deoxy-D-glucose in positron emission tomography for colorectal cancer. Eur J Nucl Med Mol Imaging 30(7):988–994
19. Herrmann K, Ott K, Buck AK, Lordick F, Wilhelm D, Souvatzoglou M et al (2007) Imaging gastric cancer with PET and the radiotracers 18F-FLT and 18F-FDG: a comparative analysis. J Nucl Med 48(12):1945–1950
20. Cobben DC, van der Laan BF, Maas B, Vaalburg W, Suurmeijer AJ, Hoekstra HJ et al (2004) 18F-FLT PET for visualization of

laryngeal cancer: comparison with 18F-FDG PET. J Nucl Med 45(2):226–231
21. Troost EG, Vogel WV, Merkx MA, Slootweg PJ, Marres HA, Peeters WJ et al (2007) 18F-FLT PET does not discriminate between reactive and metastatic lymph nodes in primary head and neck cancer patients. J Nucl Med 48(5):726–735
22. Choi SJ, Kim JS, Kim JH, Oh SJ, Lee JG, Kim CJ et al (2005) [18F]3′-deoxy-3′-fluorothymidine PET for the diagnosis and grading of brain tumors. Eur J Nucl Med Mol Imaging 32(6):653–659
23. Muzi M, Spence AM, O'Sullivan F, Mankoff DA, Wells JM, Grierson JR et al (2006) Kinetic analysis of 3′-deoxy-3′-18F-fluorothymidine in patients with gliomas. J Nucl Med 47(10): 1612–1621
24. Chen K, Bandy D, Reiman E, Huang SC, Lawson M, Feng D et al (1998) Noninvasive quantification of the cerebral metabolic rate for glucose using positron emission tomography, 18F-fluoro-2-deoxyglucose, the Patlak method, and an image-derived input function. J Cereb Blood Flow Metab 18(7):716–723
25. Pio BS, Park CK, Pietras R, Hsueh WA, Satyamurthy N, Pegram MD et al (2006) Usefulness of 3′-[F-18]fluoro-3′-deoxythymidine with positron emission tomography in predicting breast cancer response to therapy. Mol Imaging Biol 8(1):36–42
26. Kenny LM, Vigushin DM, Al-Nahhas A, Osman S, Luthra SK, Shousha S et al (2005) Quantification of cellular proliferation in tumor and normal tissues of patients with breast cancer by [18F]fluorothymidine-positron emission tomography imaging: evaluation of analytical methods. Cancer Res 65(21):10104–10112
27. Trastuzumab package insert. http://www.accessdata.fda.gov/drugsatfda_docs/label/2000/trasgen020900lb.htm. Accessed 9 Oct 2015
28. Eisenhauer EA, Therasse P, Bogaerts J, Schwartz LH, Sargent D, Ford R et al (2009) New response evaluation criteria in solid tumours: revised RECIST guideline (version 1.1). Eur J Cancer 45(2):228–247
29. Young RJ, Sills AK, Brem S, Knopp EA (2005) Neuroimaging of metastatic brain disease Neurosurgery 57(5 Suppl):S10–S23 **discusssion S1–4**
30. Cha S (2009) Neuroimaging in neuro-oncology. Neurotherapeutics 6(3):465–477
31. da Cruz LCH Jr, Rodriguez I, Domingues RC, Gasparetto EL, Sorensen AG (2011) Pseudoprogression and pseudoresponse: imaging challenges in the assessment of posttreatment glioma. AJNR Am J Neuroradiol 32(11):1978–1985
32. Li YQ, Chen P, Haimovitz-Friedman A, Reilly RM, Wong CS (2003) Endothelial apoptosis initiates acute blood-brain barrier disruption after ionizing radiation. Cancer Res 63(18):5950–5956
33. Brandsma D, Stalpers L, Taal W, Sminia P, van den Bent MJ (2008) Clinical features, mechanisms, and management of pseudoprogression in malignant gliomas. Lancet Oncol 9(5):453–461
34. Fiegler W, Langer M, Scheer M, Kazner E (1986) Reversible computed tomographic changes following brain tumor irradiation induced by the "early-delayed reaction" after radiation. Der Radiol 26(4):206–209
35. Thorsen F, Fite B, Mahakian LM, Seo JW, Qin S, Harrison V et al (2013) Multimodal imaging enables early detection and characterization of changes in tumor permeability of brain metastases. J Control Release 172(3):812–822
36. Schiepers C, Chen W, Dahlbom M, Cloughesy T, Hoh CK, Huang SC (2007) 18F-fluorothymidine kinetics of malignant brain tumors. Eur J Nucl Med Mol Imaging 34(7):1003–1011
37. Bates SE (2015) Central nervous system metastasis from breast cancer. Oncologist 20(1):3–4
38. Lin NU, Gabrail NY, Sarantopoulos J, Schwartzberg LS, Kesari S, Bates SE et al (2014) Evaluation of CNS and peripheral antitumor activity of ANG1005 in patients with brain metastases from breast tumors and other advanced solid tumors. J Clin Oncol 32:5s **(suppl; abstr 2523)**
39. FDA approves ANG1005 for the treatment of glioblastoma multiforme. http://angiochem.com/angiochem%E2%80%99s-ang1005-received-orphan-drug-designation-fda-treatment-glioblastoma-multiform. Accessed 6 Feb 2016
40. Lim E, Lin NU (2014) Updates on the management of breast cancer brain metastases. Oncology 28(7):572–578
41. Paclitaxel (Taxol) package insert data. https://www.medicines.org.uk/emc/PIL.25823.latest.pdf. Accessed 19 Aug 2015